pH-sensitivity of the ribosomal peptidyl transfer reaction dependent on the identity of the A-site aminoacyl-tRNA

Magnus Johansson[a], Ka-Weng Ieong[a], Stefan Trobro[a], Peter Strazewski[b], Johan Åqvist[a], Michael Y. Pavlov[a], and Måns Ehrenberg[a,1]

[a]Department of Cell and Molecular Biology, Biomedical Center, Uppsala University, Box 596, S-751 24 Uppsala, Sweden; and [b]Laboratoire de Synthèse de Biomolécules, Institut de Chimie et Biochimie Moléculaires et Supramoléculaires (Unité Mixte de Recherche 5246), Université Claude Bernard Lyon 1, 69622 Villeurbanne Cedex, France

Edited* by Thomas A. Steitz, Yale University, New Haven, CT, and approved November 3, 2010 (received for review August 24, 2010)

We studied the pH-dependence of ribosome catalyzed peptidyl transfer from fMet-tRNA^{fMet} to the aa-tRNAs Phe-tRNA^{Phe}, Ala-tRNA^{Ala}, Gly-tRNA^{Gly}, Pro-tRNA^{Pro}, Asn-tRNA^{Asn}, and Ile-tRNA^{Ile}, selected to cover a large range of intrinsic pK_a-values for the α-amino group of their amino acids. The peptidyl transfer rates were different at pH 7.5 and displayed different pH-dependence, quantified as the pH-value, pK_a^{obs}, at which the rate was half maximal. The pK_a^{obs}-values were downshifted relative to the intrinsic pK_a-value of aa-tRNAs in bulk solution. Gly-tRNA^{Gly} had the smallest downshift, while Ile-tRNA^{Ile} and Ala-tRNA^{Ala} had the largest downshifts. These downshifts correlate strongly with molecular dynamics (MD) estimates of the downshifts in pK_a-values of these aa-tRNAs upon A-site binding. Our data show the chemistry of peptide bond formation to be rate limiting for peptidyl transfer at pH 7.5 in the Gly and Pro cases and indicate rate limiting chemistry for all six aa-tRNAs.

ribosome | kinetics | rate limiting step | accommodation | molecular dynamics

The ribosome promotes protein elongation by transfer of the nascent peptide chain from P-site peptidyl-tRNA to A-site aminoacyl-tRNA (aa-tRNA) (Fig. 1) and translocation of messenger RNA (mRNA) and tRNAs. Peptide bond formation is initiated by a nucleophilic attack of the α-amino group of the amino acid, ester linked to the A-site tRNA, on the ester carbonyl carbon of the peptide chain linked to the 3′-oxygen of the P-site tRNA (Fig. 2). Biochemical data (1–3), crystallographic data (4–6), and molecular dynamics simulations (7, 8) have shown that the 2′OH group of A76 of the P-site tRNA greatly accelerates peptide bond formation by providing a shuttle of the proton from the attacking α-amino group to the leaving 3′O of the deacylated P-site tRNA. The rate of ribosomal peptidyl transfer is further accelerated by a network of H-bonds involving water molecules and conserved bases in the peptidyl transferase center (PTC) of the ribosome (4, 8, 9).

Peptidyl transfer requires that the α-amino group of the amino acid on the A-site tRNA is in charge neutral rather than in protonated NH_3^+ form (Fig. 2) (10). At 25 °C the pK_a-values of the α-amino groups of amino acids in bulk water range from 8.8 (Asn) to 10.6 (Pro) units (11). The pK_a-values of the aa-tRNAs, approximated by the pK_a-values of the corresponding amino acid methyl and ethyl esters (12–14), are downshifted in relation to those of the amino acids by two units, with 20 °C values ranging from 6.8 (Asn) to 8.6 (Pro) (Table 1). The rate of ribosomal peptidyl transfer might therefore be expected to vary differently with pH in the physiological range 6–8 for different A-site bound aa-tRNAs. The sensitivity of peptide bond formation to pH-variation in the 6–8 range has so far only been observed for aa-tRNA analogues but not for native aa-tRNAs (15). It has been suggested that the lack of pH sensitivity for aa-tRNAs is that their accommodation in the A site is so slow that the expected pH-sensitivity of the chemistry of peptidyl transfer is completely masked (16, 17). This view (18–21) was recently challenged in a study (22), based on an *Escherichia coli* system for protein synthesis optimized for speed and accuracy. Here the activation enthalpy and entropy for peptidyl transfer from initiator tRNA to a native aa-tRNA were similar to the corresponding activation parameters for peptidyl transfer to puromycin, lacking a rate limiting accommodation step (23). From this similarity it was argued that peptidyl transfer to native aa-tRNA and to puromycin may both be rate-limited by the chemistry of peptide bond formation (22). Indeed, incorporation rates in translation of N-alkyl aa-tRNAs (including natural Pro-tRNAs) vs. Phe- and Ala-tRNAs differ in a manner that correlates strongly with α-amino group reactivity (24–26).

Here, we studied the pH-dependence of the rate of peptidyl transfer from P-site bound initiator tRNA to six different aa-tRNAs entering the ribosome in ternary complex with EF-Tu and GTP. The aa-tRNAs were selected to cover a large range of pK_a-values for their α-amino groups (Table 1, left). We used the linear interaction energy (LIE) method (27, 28) to estimate the shift between the pK_a-values of these aa-tRNAs in bulk water and in A site.

We conclude that the chemistry of peptidyl transfer limits the rate of peptide transfer to Gly-tRNA^{Gly} and Pro-tRNA^{Pro} at physiological pH, and that a high pK_a-value of Pro-tRNA^{Pro} contributes to its small rate of peptidyl transfer (24). This result shows that the chemistry of peptide bond formation and its pH-dependence are relevant for the rate of protein elongation in the living cell and opens a window for kinetic studies of peptide bond formation on the ribosome with native tRNA substrates. The strong correlation that we observe between the molecular dynamics (MD) simulated and the kinetically estimated, apparent pK_a-shifts for the six aa-tRNAs suggests that the chemistry of peptide bond formation could, surprisingly, be rate limiting for peptidyl transfer to all six aa-tRNAs at all pH-values.

Results

pH-Dependence of the Rate of Ribosomal Peptidyl Transfer. The pK_a-values of the α-amino groups of aa-tRNAs in bulk solution, approximated by the pK_a-values of the corresponding methyl and ethyl esters (12–14), vary greatly with the amino acid side groups.

Author contributions: P.S., J.A. and M.E. designed research; M.J., K.-W.I., and S.T. performed research; P.S. and M.Y.P. contributed new reagents/analytic tools; M.J., K.-W.I., S.T., J.A., M.Y.P, and M.E. analyzed data; and M.J., J.A., and M.E. wrote the paper.

The authors declare no conflict of interest.

*This Direct Submission article had a prearranged editor.

Freely available online through the PNAS open access option.

[1]To whom correspondence should be addressed. E-mail: ehrenberg@xray.bmc.uu.se.

This article contains supporting information on-line at www.pnas.org/lookup/suppl/doi:10.1073/pnas.1012612107/-/DCSupplemental.

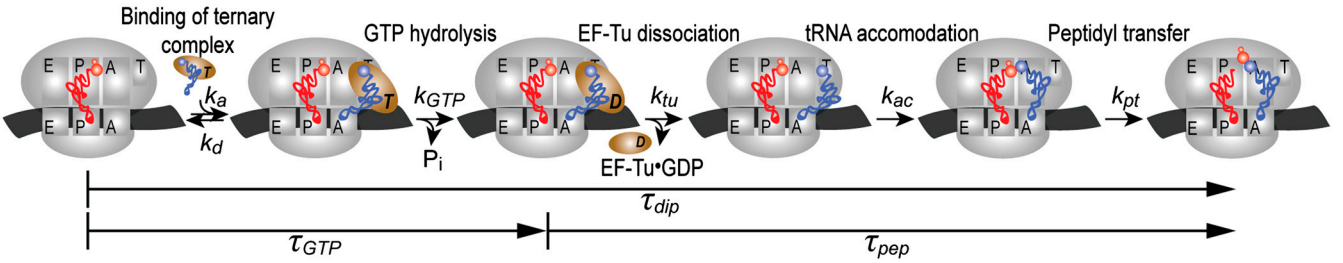

Fig. 1. Schematic representation of steps leading to ribosomal peptidyl transfer. Here, τ_{GTP} and τ_{dip} represent the average times to complete GTP hydrolysis and peptide bond formation, respectively, starting from free ternary complexes and initiated ribosomes. By subtracting τ_{GTP} from τ_{dip}, the average time for all steps subsequent to GTP hydrolysis, τ_{pep}, is obtained: $\tau_{pep} = \tau_{dip} - \tau_{GTP}$. In this scheme we have for simplicity assumed that release of EF-Tu from the ribosome precedes accommodation, so that τ_{pep} includes the time, $1/k_{tu}$. If release of EF-Tu·GDP from the ribosome occurs in parallel with accommodation (16), then $1/k_{tu}$ would not be included in τ_{pep} (See also *Data Evaluation* in *SI Text*).

We have selected six aa-tRNAs (Table 1, column 1) with bulk solution pK_a-values in the 6.8 (Asn-tRNA^{Asn}) to 8.6 (Pro-tRNA^{Pro}) pH unit interval (Table 1, column 2). The pH-dependence of the rate of ribosome catalyzed peptidyl transfer from initiator tRNA to the six aa-tRNAs was studied with quench-flow techniques.

Ternary complex, consisting of EF-Tu, [^{3}H]GTP and one of the six aa-tRNAs, was rapidly mixed in a quench-flow instrument with 70S ribosomes, containing fMet-tRNA^{fMet} ([^{3}H]Met or [^{35}S]Met) in the P site, with an empty A site programmed with either one of the codons AAC (Asn), UUU (Phe), AUC (Ile), GCA (Ala), GGC (Gly), and CCC (Pro). Each one of these codons was read by a single isoaccepting tRNA, charged with amino acid in bulk tRNA or in partially purified form (tRNA^{Phe}). After mixing, the time dependent extents of GTP hydrolysis, quantified as the ratio [^{3}H]GDP/([^{3}H]GDP + [^{3}H]GTP), and dipeptide formation, quantified as ratios [^{3}H]Met-aa/([^{3}H]Met-aa + [^{3}H]Met) or [^{35}S]Met-aa/([^{35}S]Met-aa + [^{35}S]Met), were monitored at 20 °C at pH-values in the 6–8 range. GDP was separated from GTP by TLC or HPLC and fMet from fMet-aa by RP-HPLC.

For measurement precision, GTP hydrolysis and dipeptide formation were always monitored in the *very same experiment*. The average times for GTP hydrolysis (τ_{GTP}, see *SI Text: Eq S2*) and dipeptide formation (τ_{dip}, see *SI Text: Eq S1*) and their standard errors were estimated by fitting Eqs. S4 (single exponential kinetics, *SI Text*) and S5 (double exponential kinetics, *SI Text*) to experimental data. The average time for peptidyl transfer (τ_{pep}) was estimated as the difference $\tau_{pep} = \tau_{dip} - \tau_{GTP}$, illustrated schematically in Fig. 1 and graphically as the shaded area in Fig. 3*A* and Fig. S1 (See *Data Evaluation* in *SI Text*). In all cases τ_{pep} decreased significantly when pH increased.

We have defined a "compounded" rate constant, k_{pep}, for all steps after GTP hydrolysis up to and including peptide bond formation (see Fig. 1 for details) as the inverse of τ_{pep}, i.e., $k_{pep} = 1/\tau_{pep}$. Values of k_{pep} estimated from quench-flow data at different pH-values are shown in Figs. 3 *B–G*.

In the Pro and Gly cases, plots of $\log_{10} k_{pep}$ vs. pH are linear at low pH with positive slopes close to one (Fig. 3*H*). At further pH-increase, $\log_{10} k_{pep}$ asymptotically approaches its maximal value, $\log_{10} k_{pep}^{max}$. For these two aa-tRNAs the variation of k_{pep} with pH was due to the titration of a reaction-essential group with a single proton. This group, we propose, is the α-amino group of tRNA-bound Gly or Pro in the ribosomal A site (Fig. 2). By inference, we suggest that the variation of k_{pep} with pH for all six aa-tRNAs (Fig. 3) is due to single proton titration on the α-amino group, i.e., (see *SI Text*):

$$k_{pep} = \frac{k_{pep}^{max}}{1 + 10^{(pK_a^{obs} - pH)}}. \quad [1]$$

Here pK_a^{obs} is operationally defined as the pH-value at which $k_{pep} = k_{pep}^{max}/2$. Estimates of pK_a^{obs} and k_{pep}^{max} for all six aa-tRNAs are shown in Table 1. The largest pK_a^{obs}-values are seen for Pro ($pK_a^{obs} = 7.8$) and Gly ($pK_a^{obs} = 7.4$), and the smallest for Asn ($pK_a^{obs} = 5.9$), while intermediate pK_a^{obs}-values are seen for Phe ($pK_a^{obs} = 6.1$), Ile ($pK_a^{obs} = 6.1$), and Ala ($pK_a^{obs} = 6.3$) (Table 1 and Fig. 3). The pK_a^{obs}-values are downshifted in relation to the pK_a-values for aa-tRNAs in bulk solution, pK_a^{aq}, by about one unit in the Asn, Phe, and Pro cases, 1.5 unit in the Ile and Ala cases, and 0.4 unit in the Gly case (Table 1, columns 2 and 3).

The k_{pep}^{max}-values were largest for the fast aa-tRNAs cognate to Phe ($k_{pep}^{max} = 28\ s^{-1}$), Ile ($k_{pep}^{max} = 22\ s^{-1}$), and Ala ($k_{pep}^{max} = 25\ s^{-1}$), smallest for the slow aa-tRNAs cognate to Asn ($k_{pep}^{max} = 11\ s^{-1}$) and Gly ($k_{pep}^{max} = 13\ s^{-1}$), while the classification of Pro-tRNA^{Pro} as fast or slow was uncertain due to the larger error in the estimate of k_{pep}^{max} in this case (Table 1, column 4).

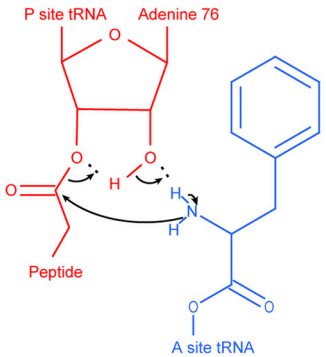

Fig. 2. The proposed mechanism of peptidyl transfer (4, 7, 8, 39). A nucleophilic attack of the α-amino group of the A-site aa-tRNA (blue, here Phe-tRNA^{Phe}) on the ester carbonyl carbon of the P-site peptidyl-tRNA (red) results in a six-membered transition state (40).

MD Simulated pK_a-Values of A-Site Bound Aminoacyl-tRNAs. In order to examine the relation between the pK_a^{obs}-values (Table 1, column 3) and the physical process of ionizing the α-amino group in the ribosomal A site, we carried out MD simulations of the

Table 1. pH dependence of k_{pep} for different aminoacyl-tRNAs at 20 °C

Aminoacyl-tRNA	pK_a^{aq} *	pK_a^{obs}	k_{pep}^{max} (s^{-1})	$k_{pep}^{pH7.5}$ (s^{-1}) †
Asn-tRNA^{Asn}	6.8	5.9 ± 0.2	11 ± 1	11 ± 1
Phe-tRNA^{Phe}	7.2	6.1 ± 0.1	28 ± 1	27 ± 1
Ile-tRNA^{Ile}	7.8	6.1 ± 0.2	22 ± 1	21 ± 1
Ala-tRNA^{Ala}	7.9	6.3 ± 0.1	25 ± 2	24 ± 1
Gly-tRNA^{Gly}	7.8	7.36 ± 0.04	13 ± 1	7.6 ± 0.2
Pro-tRNA^{Pro}	8.6	7.8 ± 0.2	17 ± 5	6.0 ± 0.5

*pK_a of the α-NH_2 group of aa-tRNA in bulk water (see *Materials and Methods*).

†k_{pep}, calculated at pH 7.5 from fits of experimental data (Fig. 3 *B–G*).

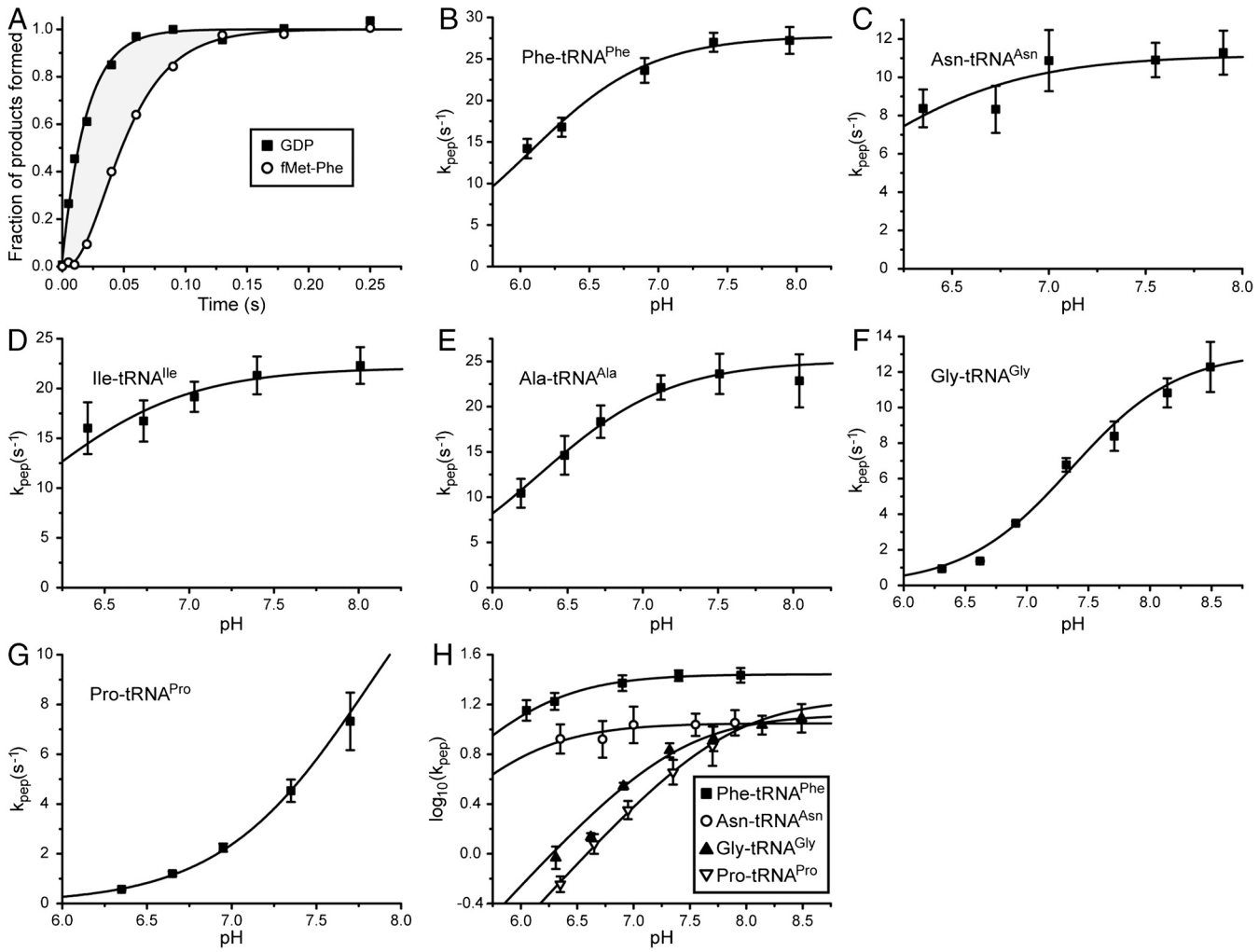

Fig. 3. pH dependence of peptidyl transfer. (*A*) The normalized amount of GDP and fMetPhe dipeptide formed as a function of time when EF–Tu·Phe–tRNA^{Phe}·[^{3}H]GTP ternary complexes react at pH 7.4 and 20 °C with f[^{35}S]Met-tRNA^{fMet} initiated 70S ribosomes displaying UUU (Phe) codon in A site. The shaded area represents the mean time, τ_{pep}, for all reaction steps subsequent to GTP hydrolysis up to and including peptidyl transfer. (*B–G*) The compounded rate constant, k_{pep}, of all reaction steps subsequent to GTP hydrolysis up to and including peptidyl transfer for different aa-tRNAs at different pH. k_{pep} is calculated as the inverse of τ_{pep} estimated from experiments as shown in *A*. The curves represent nonlinear fitting of the data to an equation where a single reacting proton is being titrated (Eq S12 in *SI Text*). Error bars represent standard deviation of the data points calculated as weighted averages from two or three independent experiments (See *Data Evaluation* in *SI Text*). (*H*) The decimal logarithm of the compounded rate constant k_{pep} for different aa-tRNAs plotted vs. pH. For Gly-tRNA^{Gly} and Pro-tRNA^{Pro} at low pH, $\log_{10}(k_{pep})$ is linear in pH with slope one, indicating titration of one proton in a reaction-essential group.

CCA end of the six different aa-tRNAs in both the neutral and protonated form in bulk water as well as on the ribosome with a dipeptide bound to the P-site tRNA (7). We used the LIE method to estimate the pK_a-shifts, $\Delta pK_a = pK_a^{ribo} - pK_a^{aq}$, of the ribosome-bound aa-tRNAs relative to their bulk solution values in terms of electrostatic and nonpolar interaction energy contributions to the neutral and ionized forms of their α-amino groups. In this model, the slope $\Delta\Delta pK_a^{calc}$ of the straight line that defines ΔpK_a from these standard energies is given by (see *SI Text*):

$$-(\mathrm{RT}\log 10)\Delta\Delta pK_a^{calc} = \alpha\Delta\Delta\langle U_{vdw}\rangle + \beta\Delta\Delta\langle U_{el}\rangle. \quad [2]$$

Here, $\Delta\Delta\langle U_{el}\rangle = \Delta\langle U_{el}\rangle_{ribo} - \Delta\langle U_{el}\rangle_{aq}$ and $\Delta\Delta\langle U_{vdw}\rangle = \Delta\langle U_{vdw}\rangle_{ribo} - \Delta\langle U_{vdw}\rangle_{aq}$, where $\Delta\langle U_{el}\rangle_{ribo}$ and $\Delta\langle U_{el}\rangle_{aq}$ are the differences in electrostatic energy between the ionized and neutral forms of ribosome-bound and free aa-tRNA, respectively, while $\Delta\langle U_{vdw}\rangle_{ribo}$ and $\Delta\langle U_{vdw}\rangle_{aq}$ are the corresponding differences for the van der Waals energy. The parameter β is a scaling constant that relates electrostatic potential energy differences to the corresponding free energies and it includes the standard linear response factor of $\frac{1}{2}$ as well as all contributions to the effective dielectric constant that are not represented by the microscopic simulation model of the PTC. $\alpha = 0.18$ is a standard scaling factor relating van der Waals potential energy differences, $\Delta\langle U_{vdw}\rangle$, to nonpolar free energy contributions [see, e.g., (29)] and $\mathrm{RT}\log 10 = 1.34$ at 20 °C.

The pK_a^{obs}-values, operationally defined from the pH-dependence of the rate, k_{pep}, of peptidyl transfer on the ribosome as described in the previous section, are all downshifted in relation to the experimentally estimated pK_a-values, pK_a^{aq}, of the α-amino groups of aa-tRNAs in bulk solution (Table 1). If the chemistry of peptidyl transfer, rather than a preceding step, is rate limiting for k_{pep} (Fig. 1), one would expect a strong correlation between pK_a-shifts calculated according to Eq. **2** above and the experimentally determined $\Delta pK_a^{obs} = pK_a^{obs} - pK_a^{aq}$ values (Table 1). If, in contrast, a step preceding the chemistry of peptidyl transfer is rate limiting for k_{pep}, no such correlation would be expected a priori.

We plotted the empirical ΔpK_a^{obs}-values for the six different aa-tRNAs vs. the MD-estimated ΔpK_a^{calc}-values for the six tRNAs

with the unknown dielectric scaling constant, β, as a fitted parameter (Fig. 4). The figure reveals a remarkably strong, positive correlation between the ΔpK_a^{calc}- and ΔpK_a^{obs}-values.

Discussion

We have studied the pH-dependence at 20 °C of the rate constant, k_{pep}, for fMet transfer from initiator tRNA in the P site to each one of six aa-tRNAs cognate to Asn, Phe, Ile, Ala, Gly, or Pro in the A site of the ribosome. k_{pep} defined as the inverse of the average time, τ_{pep}, for aa-tRNA to receive fMet after hydrolysis of GTP on EF-Tu (Fig. 1), displays distinct pH-dependence for all six tRNAs (Fig. 3 *B–G*). The pH-dependence of the peptidyl transfer reaction, quantified as the pH-value, pK_a^{obs}, at which k_{pep} is half its maximal value at high pH, k_{pep}^{max}, varies among the six aa-tRNAs by almost two pH units (Table 1, column 3). There is, at the same time, a positive correlation between the pK_a-value of the α-amino group of an aa-tRNA in bulk water (Table 1, column 2), pK_a^{aq}, and its pK_a^{obs}-value, suggesting that the pH-dependence of k_{pep} reflects inhibition of peptide bond formation due to protonation of the α-amino group of the A-site aa-tRNA. Furthermore, plots of $\log_{10} k_{pep}$ vs. pH in the Pro and Gly cases give straight lines with slopes very close to one in the low pH range (Fig. 3*H*), suggesting titration of a single proton for peptidyl transfer to Gly-tRNA^{Gly} and Pro-tRNA^{Pro} (11). From this result, we propose that titration of the α-amino groups of Gly and Pro is the sole explanation for the pH-dependence of the rate of peptidyl transfer to these aa-tRNAs (Fig. 2). Because also the pH-dependence of k_{pep} of the other four tRNAs is accounted for by single proton titrations of their α-amino groups, we suggest that the pH-dependence of k_{pep} has the same origin for all six tRNAs. It is, we suggest, not likely that this variegated spectrum of pK_a^{obs}-values and its correlation with the spectrum of pK_a^{aq}-values associated with its aa-tRNAs is caused by proton titration on any other functional group in the ribosome or by different tRNA-bodies. Yet another hypothesis, by which the rate of accommodation of aa-tRNA in the A site is severely inhibited by protonation of its amino group, so far lacks a clear mechanistic interpretation.

A distinct pH-dependence of the rate of peptidyl transfer to native aa-tRNAs in the ribosomal A site has not been observed before (15). The absence of pH-dependence has been rationalized as due to rate limiting accommodation of aa-tRNA in the A site, masking the (expected) pH-dependence of the rate constant, k_{pt} (see Fig. 1), for the chemistry of peptide bond formation (15). In fact, the pH-dependence of the peptidyl transfer reaction has previously been observed only for small aa-tRNA-analogs, like puromycin, C-puromycin, CC-puromycin (23, 30, 31), or puromycin analogs (32). For these, the pH-dependence is complex, with the effect of *two* protons on the rate of peptidyl transfer to puromycin at 37 °C (23, 30) as well as at 20 °C (31). The effect of *two* protons or one proton was observed for C-puromycin at 37 °C (30) or 20 °C (31), respectively. Furthermore, the rate of peptidyl transfer to CC-puromycin displayed a qualitatively different and much weaker pH-dependence (30).

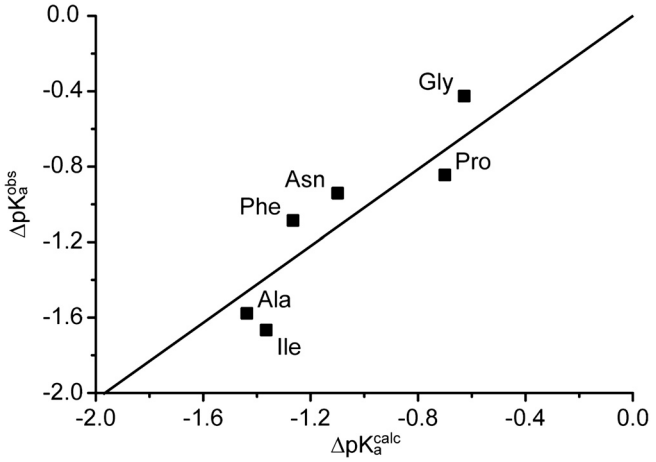

Fig. 4. Observed pK_a shifts vs. MD-simulated pK_a shifts. Experimentally observed shifts in pK_a of the α-amino group of aa-tRNAs on the ribosome relative to aa-tRNAs in bulk water, ΔpK_a^{obs}, plotted vs. MD-simulated shifts, ΔpK_a^{calc}, in the pK_a-value of aa-tRNAs as they move from bulk water to ribosomal A site.

In contrast, the present findings show that the rate constant for the chemistry of peptidyl transfer, k_{pt} in Fig. 1, can be directly assessed in kinetic experiments with native aa-tRNAs performed at pH-values below the pK_a^{obs}-values reported in Table 1: in these experimentally accessible pH-regimes the chemistry of peptidyl transfer is slower than the accommodation of aa-tRNA in the A site. An interesting question is now whether the chemistry of peptidyl transfer is slower than preceding steps on the pathway from GTP hydrolysis only at low pH-values. Or, alternatively, if also the maximal rate constant for peptide bond formation (k_{pep}^{max}) in the high pH range is rate limited by the chemistry of peptidyl transfer for some or all aa-tRNAs. The answer to this question depends on the cause of the varying downshifts of the kinetically determined pK_a^{obs}-values in relation to the pK_a^{aq}-values for aa-tRNAs in bulk water (Compare columns 2 and 3 in Table 1).

In our kinetic analysis based on average times, pK_a^{obs} is determined by the pK_a-value, pK_a^{ribo}, of the α-amino group of a ribosome-bound aa-tRNA through (*SI Text*):

$$pK_a^{obs} = pK_a^{ribo} + \log_{10}(k_{pep}^{max}/k_{pt}^{max}). \quad [3]$$

Here, k_{pt}^{max} is the high pH-limit of the rate constant, k_{pt}, for the chemistry of peptidyl transfer, i.e., when the α-amino group is neutral (Fig. 2) and k_{pep}^{max} is the corresponding high pH-limit of the compounded rate constant for all steps leading to peptidyl transfer after GTP hydrolysis on EF-Tu (Fig. 1). Eq. **3** shows that when the chemistry of peptide bond formation, k_{pt}^{max}, is rate limiting for k_{pep}^{max}, i.e., $k_{pep}^{max} \approx k_{pt}^{max}$ so that $\log_{10}(k_{pep}^{max}/k_{pt}^{max}) \approx 0$, then pK_a^{obs} is approximated by pK_a^{ribo}. When, in contrast, a step prior to the chemistry of peptide bond formation is rate limiting for k_{pep}^{max} ($k_{pt}^{max} \gg k_{pep}^{max}$) then pK_a^{obs} is much smaller than pK_a^{ribo}. In general, the downshifts, ΔpK_a^{obs}, of the pK_a^{obs}-values relative to the pK_a^{aq}-values for the amino groups of aa-tRNAs in bulk solution (Table 1) are given by:

$$\Delta pK_a^{obs} = pK_a^{obs} - pK_a^{aq} = \Delta pK_a + \log_{10}(k_{pep}^{max}/k_{pt}^{max}). \quad [4]$$

This expression shows that if a putative downshift, ΔpK_a, of the pK_a-value of the amino group of an aa-tRNA as it moves from bulk water to the A site of the ribosome, were known, the ratio $k_{pep}^{max}/k_{pt}^{max}$ could be determined from ΔpK_a^{obs}. This ratio could then be used to decide the extent to which the overall peptidyl transfer reaction is rate limited by aa-tRNA accommodation and other steps preceding the chemistry of peptide bond formation. Because ΔpK_a cannot be directly measured, we have used MD techniques and the LIE approximation (29) to estimate ΔpK_a according to Eq. **2**. When the estimated values of ΔpK_a, ΔpK_a^{calc}, are plotted vs. the ΔpK_a^{obs}-values, a strong correlation is seen (Fig. 4). The major part of the correlation stems from the electrostatic energy contribution, $\Delta\Delta\langle U_{el}\rangle$ (Fig. S2), while the nonpolar contribution $\Delta\Delta\langle U_{vdw}\rangle$ mainly affects the pK_a-shift of Phe-tRNA^{Phe}. The structural explanation for the different observed pK_a-shifts is straightforward, as judged from the average MD structures (Fig. 5). That is, water molecules are generally occluded from the volume surrounding the protonated amino group in the PTC, due to the position of the amino acid side chain

in the A site. This water occlusion leads to pK_a downshifts because desolvation destabilizes the NH_3^+ in relation to the NH_2 state (Fig. 5*A*). The only exception is Gly-tRNA^{Gly}, for which a water molecule can enter the volume normally occupied by the Cβ atom, thus providing more solvation of the amine and thus explaining why Gly had the smallest pK_a-shift (Fig. 5*B*). In the case of Pro-tRNA^{Pro}, on the other hand, because of the cyclic structure of Pro the volume is already more blocked for the side chain in bulk water than for most side chains, so that the desolvation effect in the PTC is not as pronounced and this leads to a smaller pK_a-shift than for most side chains. Also, Asn-tRNA^{Asn} is somewhat special because the side chain amide carbonyl group can form a favorable interaction (H-bond) with its protonated N terminus, thus somewhat attenuating the desolvation effect. The remaining three aa-tRNAs (Phe, Ala, and Ile) have the largest downshifts because of the lack of compensating interactions with the amino group.

Although the absolute value calibration of the MD calculations depended on a fitting of the unknown dielectric scaling constant, β, in Eq. **2** above, a straightforward interpretation of the observed downshifts, ΔpK_a^{obs}, is that they mainly reflect amino acid specific downshifts, ΔpK_a, in the pK_a-values of aa-tRNAs as they become ribosome bound. This interpretation is in line with the fact that already the unnormalized, β-independent electrostatic potential energy differences, $\Delta\Delta\langle U_{el}\rangle$, correlate significantly with the observed downshifts (Fig. S2). The correspondence of ΔpK_a^{obs} to ΔpK_a would imply that $k_{pep}^{max} \approx k_{pt}^{max}$, meaning that the chemistry of peptidyl transfer would dominate the overall rate of peptidyl transfer for all six aa-tRNAs also at high pH-values.

However, this conclusion is controversial, because it is generally assumed that accommodation of native aa-tRNAs in the A site is rate limiting for peptidyl transfer (18–21). Evidence for rate limiting A-site accommodation of aa-tRNA was originally based on stopped-flow experiments, showing that rapid mixing of EF-Tu·GTP in complex with fluorescence-labeled Phe-tRNA^{Phe} with ribosomes containing fMet-tRNA^{fMet} or deacylated tRNA^{fMet} in the P site leads to the same fast fluorescence change, interpreted as GTPase activation of EF-Tu, followed by the same slow fluorescence change, interpreted as Phe-tRNA^{Phe} accommodation in the A site. From the equivalence of the rate of the slow fluorescence change and the overall rate of peptide bond formation (k_{dip} in Fig. 1), accommodation was concluded to be rate limiting for k_{dip} (16, 17). In those (16, 17) and similar (15) experiments the k_{dip}-values were much smaller than k_{dip}-values reported by us (22), suggesting that a rate limiting accommodation step had been removed in our optimized buffer system, thereby allowing for direct kinetic studies of the chemistry of peptide bond formation. Very recent quench-flow experiments (33) now confirm the previously reported (22) large maximal values of k_{dip} at saturating ternary complex concentration. The authors (33) also performed stopped-flow experiments using fluorescence-labeled Phe-tRNA^{Phe} at a single ribosome concentration in excess over ternary complex and found a k_{dip} value identical to a fluorescence relaxation rate about five times smaller than the maximal value of k_{dip} at saturating concentration of ternary complexes. The slow fluorescence relaxation was ascribed to accommodation and the authors argued that its similarity with k_{dip} proves accommodation limited peptidyl transfer (33). However, the accommodation rate constant must always be larger than the maximal value of k_{dip}. Therefore, the observations in (33) do not support the assignment of the slow fluorescence change to the aa-tRNA accommodation step. Further experiments will be needed to define the exact contributions of aa-tRNA accommodation and the chemistry of peptide bond formation to the overall kinetics of peptidyl transfer.

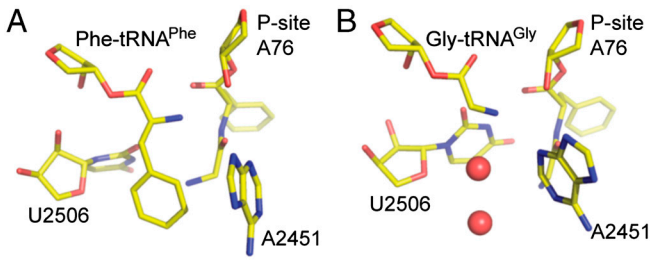

Fig. 5. Snapshots from MD simulations with Gly-Phe-tRNA^{Phe} in P site and Phe-tRNA^{Phe} (*A*) or Gly – tRNA^{Gly} (*B*) in A site. The red spheres represent water molecules.

Conclusions

We have found that ribosomal peptidyl transfer to Gly-tRNA^{Gly} and Pro-tRNA^{Pro} at pH 7.5 is rate limited by the chemistry of peptidyl transfer, rather than by a preceding step following GTP hydrolysis on EF-Tu. A straightforward interpretation of the results of our MD simulations, revealing amino acid specific downshifts of the pK_a-values of aa-tRNAs upon A-site binding, is that the chemistry of peptide bond formation is rate limiting in a pH-independent manner for all six of the studied aa-tRNAs. Resolution of the apparent contradiction between this strong conclusion from the present work and the fluorescence based conclusion that peptidyl transfer to Phe-tRNA^{Phe} is accommodation limited at physiological pH will require more detailed kinetic experiments. In any case, our results demonstrate that careful choices of pH in the 6–8 unit range open kinetic windows for direct study of the chemistry of peptide bond formation for six aa-tRNAs in an approach that is extendable to a much larger set of aa-tRNAs. Such kinetic windows are essential for characterization of the phenotypic effects of mutations in ribosomal RNA and protein with implications for cell physiology and molecular evolution.

Materials and Methods

Reagents. 70S ribosomes (*E. coli* strain MRE 600), synthetic mRNAs, initiation factors, elongation factors, and radiolabeled fMet-tRNA^{fMet} were prepared according to ref. 22 and references therein. tRNAs were from Sigma-Aldrich and Chemical Block (Russia). Radioactive compounds were from GE Healthcare and all other chemicals were from Merck or Sigma-Aldrich. All experiments were carried out in polymix buffer [95 mM KCl, 5 mM NH_4Cl, 5 mM $Mg(OAc)_2$, 0.5 mM $CaCl_2$, 8 mM putrescine, 1 mM spermidine, 5 mM potassium phosphate and 1 mM dithioerythritol (DTE)] (34).

Initiated 70S Ribosomes and Ternary Complexes. Initiated 70S ribosomes, carrying fMet-tRNA^{fMet} ([^{35}S]Met or [^{3}H]Met) in P site and displaying either of the codons UUU (Phe), CCC (Pro), AAC (Asn), GGC (Gly), GCA (Ala), or AUC (Ile) in A site, were prepared by incubating 70S ribosomes (80–85% active in dipeptide formation), fMet-tRNA^{fMet} (1.5 times the ribosome concentration), mRNA, IF1, IF3 (all in twice the ribosome concentration), and IF2 (same concentration as ribosomes) for 10 min at 37 °C. Ternary complexes were prepared by first equilibrating EF-Tu alone with [^{3}H]GDP (1:1 with EF-Tu) for 15 min at 37 °C, and then incubating it for 20 min at 37 °C in a mixture consisting of the amino acid of interest (400 μM), the corresponding aa-tRNA synthetase (2 units/μL) and tRNA (Purified tRNA^{Phe} for fMetPhe dipeptide formation, bulk tRNA in all other cases). In addition, the ribosome mix contained ATP (1 mM) and GTP (1 mM), and the ternary complex mix contained ATP (2 mM) but no extra GTP. Both mixtures contained phosphoenolpyruvate (PEP) (10 mM), pyruvate kinase (PK) (50 μg/mL), and myokinase (MK) (2 μg/mL). For the fMetPhe dipeptide experiments, where purified tRNA^{Phe} was available, the concentration of ribosomes (1 μM final) was less than the concentration of ternary complex (4 μM final), whereas in all other experiments, the concentration of ribosomes (1–2 μM final) was higher than that of ternary complex (0.5–1 μM final).

pH Adjustments. The two reaction mixtures were prepared in pH adjusted buffer. Before adding the stock ribosomes, pH of the ribosome mixture was checked (using a Hamilton Minitrode) and corrected if necessary by the addition of KOH (0.5 M) or HCl (1 M). After adding the ribosomes, pH of the two mixtures was equalized if necessary by the addition of KOH (0.5 M) or HCl (1 M) to the ternary complex mix.

Rapid Quench-Flow Experiments. The two mixtures were rapidly mixed in equal volumes in a temperature controlled quench-flow instrument (RQF-3, KinTek Corp.) as described previously (22). The quenched samples were centrifuged for 15 min at 20,800 × *g* and the [^{3}H]GTP and [^{3}H]GDP in the supernatants were separated and analyzed using either TLC (35) or a MonoQ ion-exchange column (GE Healthcare) with an on-line scint counter (βRAM3; INUS Inc.) (24). The extent of dipeptide formation was analyzed by RP-HPLC according to ref. 36.

***pK$_a$* in Bulk Water.** The *pK$_a$*-values of the α-amino group of different aa-tRNAs in solution at 20 °C were extrapolated from measured values of the *pK$_a$* of free amino acids and amino acid esters. It has previously been shown that the α-amino *pK$_a$* is very similar for tRNA-bound amino acids and more simple amino acid esters (14). From the temperature dependence of the *pK$_a$* for several amino acid methyl and ethyl esters (12, 13), the *pK$_a$* at 20 °C was calculated to between 0.10 and 0.15 units higher than at 25 °C. The *pK$_a$*s of the amino acid methyl and ethyl esters are downshifted between 2.0 and 2.2 units in relation to the corresponding amino acids (12, 13). As neither Asn nor Pro were included in the studies, we have for all six aa-tRNAs estimated the α-amino *pK$_a$* at 20 °C (Table 1) as a downshift of 2.0 units from the *pK$_a$* of free amino acids at 25 °C (11).

MD Simulations. The calculations were based on the crystallographic coordinates of the 50S *Haloarcula marismortui* ribosome with the bound peptidyl transfer transition state analog RAP, PDB code 1VQP (4). The RAP moiety was converted to an S-enantiomeric tetrahedral intermediate corresponding to CCA-Phe in the A site and CCA-Phe-Gly in the P site where the terminal amino group was kept neutral. The system was prepared using essentially the same protocols as described previously (7, 8) and consisted of all residues with atoms within 20 Å of the P-site carboxyl carbon and was solvated using the program Q (37). All Sr^{2+} ions were converted to Mg^{2+} ions and phosphate linkages and ions outside 15 Å were neutralized as described earlier. The system was relaxed to the reactant state with the aa-tRNA with a free amine in the A site and dipeptide-tRNA ester in the P site. Five additional systems were constructed in this way with A-site aa-tRNAs corresponding to the amino acids Ala, Asn, Gly, Ile, and Pro. MD simulations were performed (*SI Text*) using the program Q (37) at 300 K with the CHARMM22 force field (38).

ACKNOWLEDGMENTS. We thank Tony Forster for detailed discussions about the manuscript. This work was supported by grants from the Swedish Research Council (Project and Linné Uppsala RNA Research Center, M.E., J.Å.) and COST (European Coordination of Science and Technology) Action CM0703 on "Systems Chemistry" (P.S.).

1. Dorner S, Panuschka C, Schmid W, Barta A (2003) Mononucleotide derivatives as ribosomal P-site substrates reveal an important contribution of the 2′-OH to activity. *Nucleic Acids Res* 31:6536–6542.
2. Krayevsky AA, Kukhanova MK (1979) The peptidyltransferase center of ribosomes. *Prog Nucleic Acid Re* 23:1–51.
3. Weinger JS, Parnell KM, Dorner S, Green R, Strobel SA (2004) Substrate-assisted catalysis of peptide bond formation by the ribosome. *Nat Struct Mol Biol* 11:1101–1106.
4. Schmeing TM, Huang KS, Kitchen DE, Strobel SA, Steitz TA (2005) Structural insights into the roles of water and the 2′ hydroxyl of the P site tRNA in the peptidyl transferase reaction. *Mol Cell* 20:437–448.
5. Nissen P, Hansen J, Ban N, Moore PB, Steitz TA (2000) The structural basis of ribosome activity in peptide bond synthesis. *Science* 289:920–930.
6. Hansen JL, Schmeing TM, Moore PB, Steitz TA (2002) Structural insights into peptide bond formation. *Proc Natl Acad Sci USA* 99:11670–11675.
7. Trobro S, Åqvist J (2006) Analysis of predictions for the catalytic mechanism of ribosomal peptidyl transfer. *Biochemistry* 45:7049–7056.
8. Trobro S, Åqvist J (2005) Mechanism of peptide bond synthesis on the ribosome. *Proc Natl Acad Sci USA* 102:12395–12400.
9. Lang K, Erlacher M, Wilson DN, Micura R, Polacek N (2008) The role of 23 S ribosomal RNA residue A2451 in peptide bond synthesis revealed by atomic mutagenesis. *Chem Biol* 15:485–492.
10. Green R, Lorsch JR (2002) The path to perdition is paved with protons. *Cell* 110:665–668.
11. Fersht A (1999) *Structure and mechanism in protein science : a guide to enzyme catalysis and protein folding* (Freeman and Company, New York).
12. Hay RW, Morris PJ (1970) Proton ionization constants and kinetics of base hydrolysis of some α-amino-acid esters in aqueous solution. Part II. *J Chem Soc B* 1577–1582.
13. Hay RW, Porter LJ (1967) Proton ionization constants and kinetics of base hydrolysis of some α-amino-acid esters in aqueous solution. *J Chem Soc B* 1261–1264.
14. Wolfenden R (1963) The mechanism of hydrolysis of amino acyl Rna. *Biochemistry* 2:1090–1092.
15. Bieling P, Beringer M, Adio S, Rodnina MV (2006) Peptide bond formation does not involve acid-base catalysis by ribosomal residues. *Nat Struct Mol Biol* 13:423–428.
16. Pape T, Wintermeyer W, Rodnina MV (1998) Complete kinetic mechanism of elongation factor Tu-dependent binding of aminoacyl-tRNA to the A site of the *E. coli* ribosome. *Embo J* 17:7490–7497.
17. Rodnina MV, Fricke R, Wintermeyer W (1994) Transient conformational states of aminoacyl-tRNA during ribosome binding catalyzed by elongation factor Tu. *Biochemistry* 33:12267–12275.
18. Schmeing TM, Voorhees RM, Kelley AC, Gao YG, Murphy FVt (2009) The crystal structure of the ribosome bound to EF-Tu and aminoacyl-tRNA. *Science* 326:688–694.
19. Ledoux S, Uhlenbeck OC (2008) Different aa-tRNAs are selected uniformly on the ribosome. *Mol Cell* 31:114–123.
20. Beringer M, Rodnina MV (2007) The ribosomal peptidyl transferase. *Mol Cell* 26:311–321.
21. Zaher HS, Green R (2009) Fidelity at the molecular level: lessons from protein synthesis. *Cell* 136:746–762.
22. Johansson M, Bouakaz E, Lovmar M, Ehrenberg M (2008) The kinetics of ribosomal peptidyl transfer revisited. *Mol Cell* 30:589–598.
23. Katunin VI, Muth GW, Strobel SA, Wintermeyer W, Rodnina MV (2002) Important contribution to catalysis of peptide bond formation by a single ionizing group within the ribosome. *Mol Cell* 10:339–346.
24. Pavlov MY, Watts RE, Tan Z, Cornish VW, Ehrenberg M (2009) Slow peptide bond formation by proline and other N-alkylamino acids in translation. *Proc Natl Acad Sci USA* 106:50–54.
25. Watts RE, Forster AC (2010) Chemical models of peptide formation in translation. *Biochemistry* 49:2177–2185.
26. Zhang B, Tan Z, Dickson LG, Nalam MN, Cornish VW (2007) Specificity of translation for N-alkyl amino acids. *J Am Chem Soc* 129:11316–11317.
27. Marelius J, Hansson T, Åqvist J (1998) Calculation of ligand binding free energies from molecular dynamics simulations. *Int J Quantum Chem* 69:77–88.
28. Åqvist J, Medina C, Samuelsson JE (1994) A new method for predicting binding affinity in computer-aided drug design. *Protein Eng* 7:385–391.
29. Carlsson J, Boukharta L, Aqvist J (2008) Combining docking, molecular dynamics and the linear interaction energy method to predict binding modes and affinities for non-nucleoside inhibitors to HIV-1 reverse transcriptase. *J Med Chem* 51:2648–2656.
30. Beringer M, Rodnina MV (2007) Importance of tRNA interactions with 23 S rRNA for peptide bond formation on the ribosome: studies with substrate analogs. *Biol Chem* 388:687–691.
31. Brunelle JL, Youngman EM, Sharma D, Green R (2006) The interaction between C75 of tRNA and the A loop of the ribosome stimulates peptidyl transferase activity. *RNA* 12:33–39.
32. Okuda K, Seila AC, Strobel SA (2005) Uncovering the enzymatic pKa of the ribosomal peptidyl transferase reaction utilizing a fluorinated puromycin derivative. *Biochemistry* 44:6675–6684.
33. Wohlgemuth I, Pohl C, Rodnina MV (2010) Optimization of speed and accuracy of decoding in translation. *Embo J* 29:3701–3709.
34. Jelenc PC, Kurland CG (1979) Nucleoside triphosphate regeneration decreases the frequency of translation errors. *Proc Natl Acad Sci USA* 76:3174–3178.
35. Bilgin N, Claesens F, Pahverk H, Ehrenberg M (1992) Kinetic properties of *Escherichia coli* ribosomes with altered forms of S12. *J Mol Biol* 224:1011–1027.
36. Pavlov MY, Freistroffer DV, MacDougall J, Buckingham RH, Ehrenberg M (1997) Fast recycling of *Escherichia coli* ribosomes requires both ribosome recycling factor (RRF) and release factor RF3. *EMBO J* 16:4134–4141.
37. Marelius J, Kolmodin K, Feierberg I, Åqvist J (1998) Q: a molecular dynamics program for free energy calculations and empirical valence bond simulations in biomolecular systems. *J Mol Graph Model* 16:213–225–261.
38. MacKerell AD, Wiorkiewicz-Kuczera J, Karplus M (1995) An all-atom empirical energy function for the simulation of nucleic acids. *J Am Chem Soc* 117:11946–11975.
39. Schmeing TM, Huang KS, Strobel SA, Steitz TA (2005) An induced-fit mechanism to promote peptide bond formation and exclude hydrolysis of peptidyl-tRNA. *Nature* 438:520–524.
40. Changalov MM, Ivanova GD, Rangelov MA, Acharya P, Acharya S (2005) 2′/3′-O-peptidyl adenosine as a general base catalyst of its own external peptidyl transfer: implications for the ribosome catalytic mechanism. *Chembiochem* 6:992–996.